Fluid Dynamics & Materials Processing

Tech Science Press

Doi:10.32604/fdmp.2025.062737

ARTICLE

Performance Analysis of Foamed Fracturing Fluids Based on Microbial Polysaccharides and Surfactants in High-Temperature and High-Salinity Reservoirs

Zhiqiang Jiang[1], Zili Li[1], Bin Liang[2], Miao He[1], Weishou Hu[3], Jun Tang[3], Chao Song[4] and Nanxin Zheng[5,*]

[1]Oil & Gas Technology Research Institute, PetroChina Changqing Oilfield Company, Xi'an, 710018, China
[2]Petrochina Jilin Oilfield Company, Songyuan, 138000, China
[3]Sixth Gas Production Plant PetroChina Changqing Oilfield Company, Yan'an, 716009, China
[4]CCDC Changqing Downhole Technology Company, Xi'an, 710018, China
[5]National Key Laboratory of Oil and Gas Reservoir Geology and Exploitation, Southwest Petroleum University, Chengdu, 610500, China

*Corresponding Author: Nanxin Zheng. Email: 202114000006@swpu.edu.cn

Received: 26 December 2024; Accepted: 14 March 2025; Published: 30 June 2025

ABSTRACT: Microbial polysaccharides, due to their unique physicochemical properties, have been shown to effectively enhance the stability of foam fracturing fluids. However, the combined application of microbial polysaccharides and surfactants under high-temperature and high-salinity conditions remain poorly understood. In this study, we innovatively investigate this problem with a particular focus on foam stabilization mechanisms. By employing the Waring blender method, the optimal surfactant-microbial polysaccharide blends are identified, and the foam stability, rheological properties, and decay behavior in different systems under varying conditions are systematically analyzed for the first time. The results reveal that microbial polysaccharides significantly enhance foam stability by improving the viscoelasticity of the liquid films, particularly under high-salinity and high-temperature conditions, leading to notable improvements in both foam stability and sand-carrying capacity. Additionally, scanning electron microscopy (SEM) is used to observe the microstructure of the foam liquid films, demonstrating that the network structure formed by the foam stabilizer within the liquid film effectively inhibits foam coarsening. The Lauryl betaine and Diutan gum blend (LAB+MPS04) exhibits outstanding foam stability, superior sand-carrying capacity, and minimal core damage, making it ideal for applications in enhanced production and reservoir stimulation of unconventional reservoirs.

KEYWORDS: Foam fracturing fluid; microbial polysaccharides; synergistic effect; stabilization mechanism; performance

1 Introduction

According to the International Energy Outlook 2020 published by the International Energy Agency (IEA), global energy consumption is projected to increase by over 50% by 2050 compared to 2020 levels [1,2]. As of 2020, oil and natural gas accounted for approximately 55% of global energy consumption, and this share is expected to remain above 50% by 2050. This indicates that oil and gas will continue to play a dominant role in the global energy mix over the next three decades. As many conventional oil and gas reservoirs enter the high-water-cut and high-recovery-rate phases, unconventional reservoirs are becoming increasingly important as alternative sources of production [3,4]. However, unconventional reservoirs often exhibit low

porosity and permeability, necessitating specialized enhanced recovery techniques to achieve commercially viable extraction rates [5,6]. Among these techniques, hydraulic fracturing has emerged as a key technology for unlocking unconventional hydrocarbon resources [7]. Hydraulic fracturing involves injecting high-viscosity fracturing fluids into a well at high pressure, exceeding the formation's absorption capacity. This process generates elevated downhole pressure [8]. When the pressure surpasses the fracture threshold of the formation rock, fractures are induced, creating new pathways for hydrocarbons to flow. Continuous injection of proppant-laden fluids, such as quartz sand, ensures that these fractures remain open, thereby improving the reservoir's permeability. Once pumping ceases, the formation retains fractures of sufficient length, width, and height, allowing oil and gas to flow more freely into the wellbore and significantly enhancing well productivity [9,10]. Fracturing fluids are a critical component of hydraulic fracturing operations. A variety of fracturing fluids are currently in use, including slickwater fracturing fluids [11], conventional guar gum-based fluids [12], energized water fracturing fluids [13], and viscoelastic surfactant fluids [14]. Regardless of their specific formulations, all these fluids require large volumes of water mixed with complex additives. In the hydraulic fracturing of unconventional reservoirs, water consumption can be substantial. For instance, in the Changning-Weiyuan block of Sichuan Province, China, the average water consumption per well is approximately 25,000 m^3. Such extensive water usage can exert significant pressure on local water resources and ecosystems, raising environmental concerns about long-term sustainability.

Foam is a dispersion of gas in a liquid phase. It is widely used in both daily life and industry, such as in personal care products [15], foam firefighting [16,17], and froth flotation [18]. The most notable characteristic of foam fracturing fluids is that they require only 10%–30% of the water volume needed by conventional water-based fracturing fluids, making them highly suitable for water-scarce regions. The earliest report on foam fracturing technology appeared in 1968, when it was first applied to the development of shale reservoirs in Lincoln County, West Virginia, USA, with the foam quality controlled at 83%–85% during operations. In April 1974, Blauer et al. [19,20] published research on the frictional pressure drop in foam flow through pipes. In October of the same year, Blauer et al. further reported on the properties of foam fracturing fluids, including fluid loss, rheology, and proppant transport, as well as their field application [21], which significantly advanced the early development of foam fracturing technology. Subsequently, foam fracturing enhancement technology began to be promoted in the United States due to its low water consumption, low fluid loss, good flowback performance, and clean characteristics, and it also expanded to Canada. Although foam fracturing fluids exhibit excellent properties, foam systems are thermodynamically unstable. Over time, the performance of the foam can significantly decrease, and even collapse. Therefore, stabilizers must be added to inhibit foam decay. Extensive research has been conducted in this area, including the introduction of nanoparticles and polymers to enhance foam stability, thereby meeting design requirements. Sun et al. [22] investigated the effect of partially hydrophobic modified silica nanoparticles (SiO_2) on the stability of sodium dodecyl sulfate (SDS) foam. The study showed that, at appropriate concentrations, SiO_2 nanoparticles and SDS exhibit a synergistic effect, enhancing foam stability compared to pure SDS solutions. SiO_2/SDS dispersions generate more stable foam, primarily because the nanoparticles adsorb on the liquid film surface, increasing interfacial dilational elasticity and thus improving foam stability. AlYousef et al. [23] evaluated the potential of silica nanoparticles to enhance the stability of non-ionic surfactant foams. The results indicated that the concentration of surfactants and nanoparticles is a critical parameter for foam stability, and there exists a specific concentration range that generates more stable foam. The balance between the concentrations of non-ionic surfactants and nanoparticles can enhance foam stability by forming flocs in the solution. At a fixed surfactant concentration, adding low to medium concentrations of nanoparticles can produce more stable foam compared to surfactant alone. Rafati et al. [24] studied the interactions between solid particles in reservoirs and water-foam, to assess foam stability. They found that

the presence of solid particles significantly affects foam stability, with the impact depending on the particles' density, shape, size, and wettability. Specifically, certain particles can form monolayers, bilayers, or network structures, stabilizing the foam's liquid film, while other particles may lead to foam structure disruption. The large surface area of nanoparticles is a key reason for their ability to enhance foam stability [25–27]. However, in reservoir conditions, foam systems often face high temperatures and high salinity, under which nanoparticles can easily aggregate and lose their effectiveness [28]. Moreover, the poor biocompatibility of modified nanoparticles can result in serious environmental impacts. Microbial polysaccharides are high-molecular-weight biopolymers produced by bacteria, fungi, and cyanobacteria during their metabolic processes, providing protection to the microorganisms [29–30]. They are increasingly gaining attention due to their ease of extraction, wide availability, and broad functional range [31]. Microbial polysaccharides possess unique physicochemical properties, which also make them highly effective in stabilizing foams [32]. Kang et al. [33] used three microbial polysaccharides as foam stabilizers in AFFF. They conducted multiple analyses to explore the influence of polysaccharides on the viscosity, surface tension, foaming ability, and foam stability of AFFF solutions. This is primarily due to the increased viscosity provided by microbial polysaccharides, which enhances the surface strength of the foam liquid film and reduces the diffusion of water within the liquid film, thereby significantly slowing down the drainage rate and bubble coarsening process of the foam. Pu et al. [34] combined rheological and surface properties to study the impact of different polymers on foam stability, analyzing the stability from a microscopic perspective. Their results indicated that the liquid drainage height of polymer-enhanced foam is highly dependent on the solution viscosity at high shear rates (200 s^{-1}), rather than the initial thickening ability of the polymer. The stability of the liquid film is improved by increasing the solution's elasticity, enhancing interfacial viscoelasticity, or reducing surface tension. Verma et al. [35] used the Warrior-Blender method to investigate the foam stability of α-olefin sulfonate (AOS) in solutions containing partially hydrolyzed polyacrylamide (HPAM) or xanthan gum (XG). For different total concentrations and surfactant concentrations, the half-life of AOS-XG foam was longer than that of AOS-HPAM foam. This is mainly because the polymer concentration of HPAM or XG increases the viscoelasticity of the bulk solution and the liquid film, with XG having a stronger ability to enhance the viscoelasticity of the liquid film compared to HPAM. Therefore, AOS-XG foam exhibits better foam stability. Tiong et al. [36] investigated the synergistic effects between xanthan gum and sodium dodecyl sulfate (SDS) and cetyltrimethylammonium bromide (CTAB). The results showed that the addition of xanthan gum increased the foam liquid drainage half-life by 50,000 times. Xu et al. [37] studied the effects of welan gum and xanthan gum on in-situ foam performance and the foam stabilization mechanism. The results indicated that welan gum, through the alignment of its adjacent double-helix structure in the zipper model, forms an interconnected network structure. This structure interacts with surfactants in the liquid film, enhancing foam stability at high temperatures. In summary, using microbial polysaccharides as foam stabilizers to improve the foam stability of solutions is feasible. Compared to other foam stabilizers, microbial polysaccharides are derived from natural sources and are renewable resources, offering biocompatibility and biodegradability, making them environmentally friendly and possessing significant potential for development and application. Microbial polysaccharides, as a promising research topic, exhibit a wide variety of types, and the synergistic effects [38], temperature tolerance, and salt resistance vary among different types of microbial polysaccharides and surfactants. In the process of oil extraction, the high temperature and high salinity conditions in the reservoir environment inevitably cause the failure of many organic materials, which significantly impacts extraction efficiency [39]. Research on the foam stability behavior of materials under high temperature and high salinity conditions is of great importance. However, current studies have yet to clarify the synergistic foam stabilization mechanism of microbial polysaccharides and different types of surfactants at low concentrations under high-temperature and high-mineralization conditions in the reservoir. Therefore, it is necessary to explore in-depth the interactions between microbial polysaccharides

and surfactants, as well as their impact on foam stability, and to systematically assess the foam characteristics of microbial polysaccharide foams under varying temperature and salinity conditions. This research will not only enhance the understanding of foam behavior in extreme environments but also provide a theoretical basis and technical support for the application of microbial polysaccharide foams in unconventional oil and gas reservoirs.

In this study, various types of microbial polysaccharides were first blended with different surfactants. The optimal foam system, characterized by thermal and salt stability, was selected based on the comprehensive foam performance. The interaction mechanisms between the microbial polysaccharides and surfactants were then analyzed. Next, based on the optimal system, the foam decay characteristics and rheological properties were examined to elucidate the foam-stabilizing mechanisms of microbial polysaccharide-based foams. The microstructure of the liquid film was observed using environmental scanning electron microscopy (SEM). Finally, the foam's proppant-carrying capacity and its potential for formation damage were evaluated. The aim of this study is to optimize the stability and performance of foam fracturing fluids, particularly under high-temperature and high-salinity conditions, by exploring the synergistic effects of microbial polysaccharides and surfactants. This research addresses the challenge of poorly understood foam stabilization mechanisms in microbial polysaccharide and surfactant blends, while also enhancing foam sand-carrying capacity and reducing potential damage. Ultimately, it provides a viable technical solution for the efficient exploitation of unconventional reservoirs.

2 Experiment and Methods

2.1 Materials

Six surfactants and four microbial polysaccharides were selected in this study. Detailed information is provided in Table 1. All solutions were prepared using deionized water.

Table 1: Materials used in the experiments

Name	Abbreviation	Purity (%)	Supplier
Xanthan gum	MPS01	99%	Shandong Fengtai Biotechnology Co., Ltd. (Jinan, Shandong, China)
Welan gum	MPS02	99%	Shandong Fengtai Biotechnology Co., Ltd. (Jinan, China)
Gellan gum	MPS03	99%	Shandong Fengtai Biotechnology Co., Ltd. (Jinan, China)
Diutan gum	MPS04	99%	Shandong Fengtai Biotechnology Co., Ltd. (Jinan, China)
Sodium Dodecyl Sulfate	SDS	99%	Aladdin (Shanghai, China)
Sodium dodecylbenzenesulfonate	SDBS	99%	Aladdin
Sodium fatty alcohol polyoxyethylene ether sulfate	AES	99%	Aladdin
Sodium laureth sulfate	SLES	99%	Aladdin
Cocamidopropyl betaine	CAB	99%	Aladdin
Lauryl betaine	LAB	99%	Aladdin
Na_2SO_4	/	99%	Aladdin
$NaHCO_3$	/	99%	Aladdin
NaCl	/	99%	Aladdin

(Continued)

Table 1 (continued)

Name	Abbreviation	Purity (%)	Supplier
$CaCl_2$	/	99%	Aladdin
$MgCl_2$	/	99%	Aladdin
Na_2SO_4	/	99%	Aladdin

2.2 Methods

2.2.1 Optimization of Temperature and Salinity Resistant Foam Fracturing Fluid System

Surfactant solutions with concentrations of 0.2, 0.4, 0.6, 0.8, and 1.0 wt% were prepared, with 0.08 wt% microbial polysaccharide added to each solution. Four milliliters of the foaming liquid were injected into sample bottles, and foam was generated using a foaming device according to the Waring-Blender method, with a stirring time of 2 min. Immediately after foaming, the samples were placed in a custom-designed high-temperature foam evaluation instrument to measure the foam drainage half-life and foam expansion height. These measurements were conducted at 70°C and 80°C, and the optimal foam system was selected based on the comprehensive foam performance. Next, for the selected temperature-resistant foam system, the mineralization degree of the solution was adjusted to 30, 60, and 90 g/L. The comprehensive foam value was measured again using the same method to determine the optimal foam fracturing fluid system. Each experiment was repeated three times, with the error not exceeding 5%. The experimental setup is shown in Fig. 1.

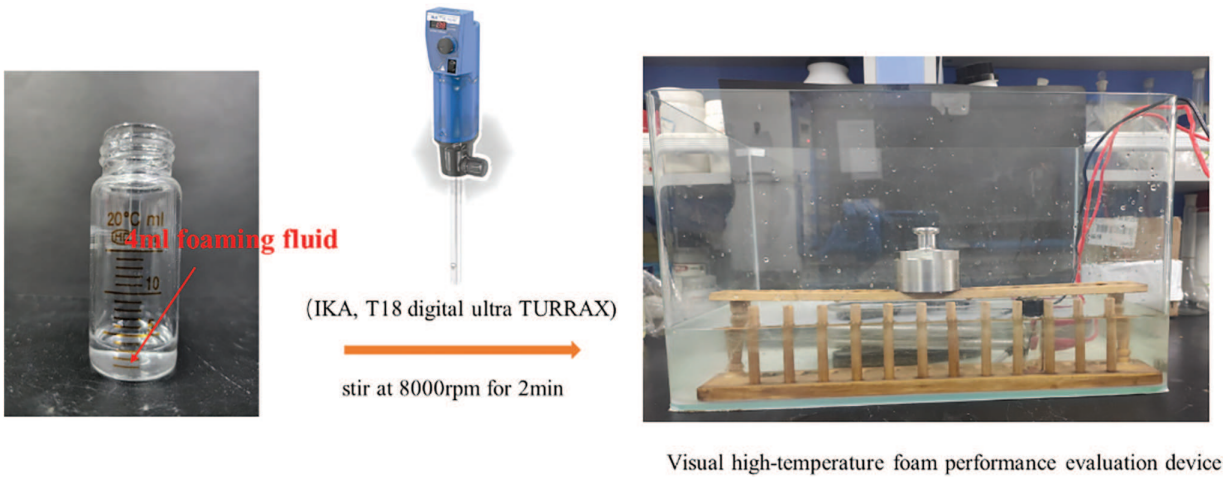

Figure 1: Illustration of the experimental apparatus

2.2.2 Performance Testing of Foam Fracturing Fluids

Static Sand Suspension Test

Repare 100 mL of the optimal system in steel cups and add 10% by volume of proppant to each. After the mixture is allowed to foam, quickly transfer it to a 500 mL graduated cylinder. Use a camera to take photos every 5 min, and record the settling behavior of the proppant in the foam system and the liquid separation from the foam over a period of 1 h. Each experiment was repeated three times, and the average value was taken as the final experimental result.

Dynamic Sand-carrying Capacity Test

Using a visual dynamic sand-carrying apparatus (Fig. 2), the foamed base liquid was mixed with the proppant and allowed to foam. The mixture was then injected into a flat plate from the left end and allowed to flow out from the right end. The proppant used was 20/40 mesh ceramic beads, with a sand ratio of 10%.

Figure 2: Dynamic sand-carrying device

Core Damage Test

The damage to core permeability by the fracturing fluid was evaluated using a core flooding apparatus (Fig. 3). Sandstone cores with a diameter of 25 ± 0.4 mm and a length of 50 ± 0.4 mm were selected for the experiment, and the temperature was set to 80°C. Core damage was assessed based on the comparison of the core permeability to N_2 before and after contact with the fracturing fluid. The equations for core permeability and core damage rate are given in Eqs. (1) and (2), respectively:

$$K = \frac{2P_0 Q\mu L}{\left(P_1^{\,2} - P_2^{\,2}\right) A} \times 1000 \tag{1}$$

where K is the permeability, mD; Q is the gas flow rate, cm^3/s; μ is the gas viscosity, mPa·s; L is the length of the core, cm; P_1 and P_2 are the inlet and outlet pressures, MPa; A is the cross-sectional area of the core, cm^2; and P_0 is the atmospheric pressure, MPa.

$$\eta_d = \frac{K_1 - K_2}{K_1} \times 100\% \tag{2}$$

where η_d is the ratio of permeability reduction to the initial core permeability, %; K_1 is the initial core permeability, mD; K_2 is the core permeability after contact with the gel-breaking fluid, mD.

Figure 3: Core flooding apparatus

2.2.3 Stabilization Mechanism of Foam Fracturing Fluid

Foam Coarsening

The foam after generation was placed on a microscope slide, and the changes in foam size and foam count were observed under a microscope at 100× magnification. Image processing software was used to analyze the variations in foam size and foam count over time before and after the addition of a foam stabilizer. Each experiment was repeated three times, and the average value was taken as the final experimental result.

Foam Microstructure

The microstructure of the foam was studied using cryo-SEM (Quanta 450, FEI Company, Hillsboro, OR, USA). Foam containing a foam stabilizer was dropped onto a groove of a copper plate with a conductive strip. The copper plate was then placed into a vacuum chamber and liquid nitrogen was introduced to maintain the temperature at −90°C. After freezing the foam, the sample surface was sputter-coated with gold to make it conductive, and the microstructure of the foam was observed using the Environmental Scanning Electron Microscope.

Foam Viscoelasticity

Foam was produced using a Waring-Blender method, and its viscoelastic properties were measured with a HAAKE MARS III rotational rheometer, both in the presence and absence of a foam stabilizer. The frequency range for scanning was between 0.01 and 30.00 Hz, and a fixed stress of 1 Pa was applied.

2.2.4 Methodology Features and Validation Process

Peculiarity of the Methods

The unique contribution of this research lies in the synergistic combination of microbial polysaccharides and surfactants for foam stabilization under extreme high-temperature and high-salinity conditions. We also elaborated on the use of the Waring blender method to create stable foam systems and analyzed their rheological properties, foam decay behaviors, and performance under various conditions. This allows for a comprehensive understanding of how microbial polysaccharides enhance foam stability and sand-carrying capacity in unconventional reservoir conditions.

Validation of Methods

To ensure the robustness and validation of our methods, we employed several validation techniques, including:

Foam performance testing: We evaluated foam generation and stability under different temperatures (70°C and 80°C) and salinities (30, 60, and 90 g/L). This multi-condition testing ensures that our methods are robust across a range of relevant reservoir conditions.

Proppant suspension and core damage tests: These were performed to validate the real-world application of the foam system, specifically its sand-carrying capacity and its impact on core permeability. We compared the performance of the microbial polysaccharide-based foam system against conventional guar gum fracturing fluids to demonstrate its superior performance.

Scanning electron microscopy (SEM): This was used to observe the microstructure of the foam liquid films, which provided insight into the network structure formed by the foam stabilizer and confirmed the stability enhancement mechanisms.

Data Set Limitations

Field applicability: Our experiments were conducted under controlled laboratory conditions that may not fully replicate the complexities of field environments. The impact of contaminants (e.g., oil phases, CO_2, SO_2) on foam stability in real reservoirs needs further investigation, as these factors could potentially affect foam performance.

Scalability: Although the results are promising at the laboratory scale, scaling up to industrial applications in larger reservoirs requires more research. Variability in field conditions, such as temperature fluctuations and mineral content, may influence foam behavior.

Polysaccharide degradation: The long-term stability of microbial polysaccharides in the harsh conditions of high-temperature, high-salinity reservoirs is not fully understood. Their degradation over time may limit their effectiveness for sustained production. Future studies will need to focus on the degradation kinetics and long-term behavior of microbial polysaccharides in such environments.

3 Results and Discussion

3.1 System Optimization

3.1.1 Optimization of Temperature Resistance

Microbial polysaccharides are environmentally friendly fermentation products and are considered renewable resources. Their use as additives in foam fracturing fluids aligns with the principles of green and sustainable development. Furthermore, these polysaccharides are low-cost and easy to store and transport, making them highly promising for widespread application in fracturing operations. In this study, we selected four different types of microbial polysaccharides, each blended with surfactants, and performed foam stability tests at 70°C and 80°C. However, since microbial polysaccharides are typically negatively charged, they can interact electrostatically with cationic surfactants, resulting in compatibility issues. As a result, we focused on evaluating the compatibility of microbial polysaccharides with anionic, anionic-nonionic, and zwitterionic surfactants. To assess foam generation and stability, the overall foam value was used as the evaluation metric. The calculation method for the comprehensive foam value is given in Eq. (3) [40–42].

$$V_t = V \times t_{1/2} \tag{3}$$

where V_t is the overall foam value, with units of mL·s; V is the foam generation volume, with units of mL; and $t_{1/2}$ is the foam drainage half-life, with units of s.

Anionic surfactants, known for their simple synthesis, low cost, and non-toxicity, are widely used in foaming fracturing fluids [43]. In this study, we investigated common anionic surfactants in combination with microbial polysaccharides to optimize the best formulations suitable for temperatures of 70°C and 80°C, based on the comprehensive foam value. Both anionic surfactants and microbial polysaccharides carry negative charges, and thus their synergistic effects are often unrelated to electrostatic interactions but are primarily attributed to non-covalent interactions between the hydrophilic groups and the microbial polysaccharide molecules. As shown in Fig. 4, the foam performance of SDS (Sodium Dodecyl Sulfate) and SDBS (Sodium Dodecyl Benzene Sulfonate) when combined with different microbial polysaccharides is presented. It is evident that the combination of SDS and MPS04 (Microbial Polysaccharide MPS04) significantly enhances the overall foam value. Specifically, at 70°C, the overall foam value of the 0.6 wt% SDS + 0.08 wt% MPS04 system reaches 21,400 mL·s, which is much higher than other anionic surfactant and microbial polysaccharide combinations. This indicates the strongest synergistic effect between SDS and MPS04. We attribute this primarily to the unique molecular structure of SDS, its high hydrophilic-lipophilic balance (HLB) value, the excellent synergistic effect with MPS04, and its superior interfacial adsorption

capacity. SDS is a linear surfactant molecule that can easily form orderly arrangements at the gas-liquid interface, thereby more effectively reducing interfacial tension and promoting foam formation and stability. In contrast, SDBS contains a benzene ring in its molecular structure, leading to less orderly arrangements at the gas-liquid interface and a poorer reduction in interfacial tension. Furthermore, the HLB value of SDS is approximately 40, making it a strongly hydrophilic surfactant that can form tighter interactions with MPS04, increasing the viscosity of the aqueous phase and the elasticity of the foam lamellae, thus enhancing foam stability. SDBS has a lower HLB value, leading to weaker interactions with MPS04 and lower viscosity and lamellae elasticity of the system. Additionally, studies have shown that SDS exhibits high adsorption rates and amounts at the gas-liquid interface, rapidly forming a stable interfacial film and further enhancing foam stability. In comparison, SDBS has a weaker interfacial adsorption capacity, resulting in less stable interfacial films and shorter foam half-time. These factors collectively contribute to the significantly better foam stabilization effect of the SDS+MPS04 system compared to the SDBS+MPS04 system.

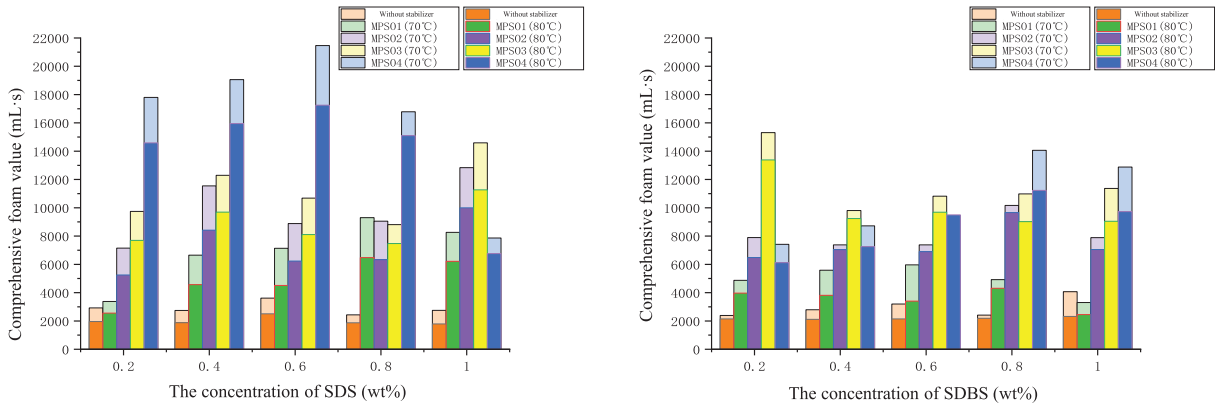

Figure 4: The comprehensive foam value of an anionic surfactant foam system varies with the surfactant concentration and the type of microbial polysaccharide

By incorporating EO (ethylene oxide) groups into the hydrophilic moiety of conventional anionic surfactants, anionic-nonionic surfactants can be obtained. Compared with traditional anionic surfactants, anionic-nonionic surfactants exhibit stronger salt tolerance. AES (Alkyl Ether Sulfate) and SLES (Sodium Lauryl Ether Sulfate) are the most widely used anionic-nonionic surfactants in the petroleum industry; therefore, we conducted a detailed study on AES and SLES. As shown in Fig. 5, it presents the foam generation and foam stability of anionic-nonionic surfactants AES and SLES when compounded with MPS04 (Microbial Polysaccharide 04). It can be observed that the addition of microbial polysaccharides significantly enhances the stability of AES and SLES foams, whether at 70°C or 80°C. Notably, the interaction between AES and microbial polysaccharides is markedly stronger than that between SLES and microbial polysaccharides. This is primarily attributed to the longer polyethylene oxide chain of AES, which not only increases its hydrophobic segment, allowing it to interact more effectively with the hydrophobic regions of MPS04, but also enhances its solvation in aqueous solutions, enabling AES to disperse more uniformly and increase the opportunity for contact with microbial polysaccharides, thus forming tighter complexes. Simultaneously, the more flexible molecular conformation of AES allows it to better adapt to the polysaccharide chains of MPS04, further enhancing the stability of the complexes through entanglements and hydrogen bonding. Additionally, the longer polyethylene oxide chain of AES reduces its surface charge density to some extent, decreasing the electrostatic repulsion with MPS04 and making their interactions more favorable. In contrast, SLES has a shorter polyethylene oxide chain, resulting in weaker hydrophobicity, poorer solvation, and lower molecular

flexibility, as well as a higher charge density, leading to relatively weaker interactions with MPS04, and thus demonstrating inferior thickening effects and stability in aqueous solutions compared to the AES-MPS04 combination. Based on the comprehensive foam value and the optimization of microbial polysaccharide types and concentrations, the optimal formulation of microbial polysaccharides and anionic-nonionic surfactants was determined to be: 0.6 wt% AES + 0.08 wt% MPS04.

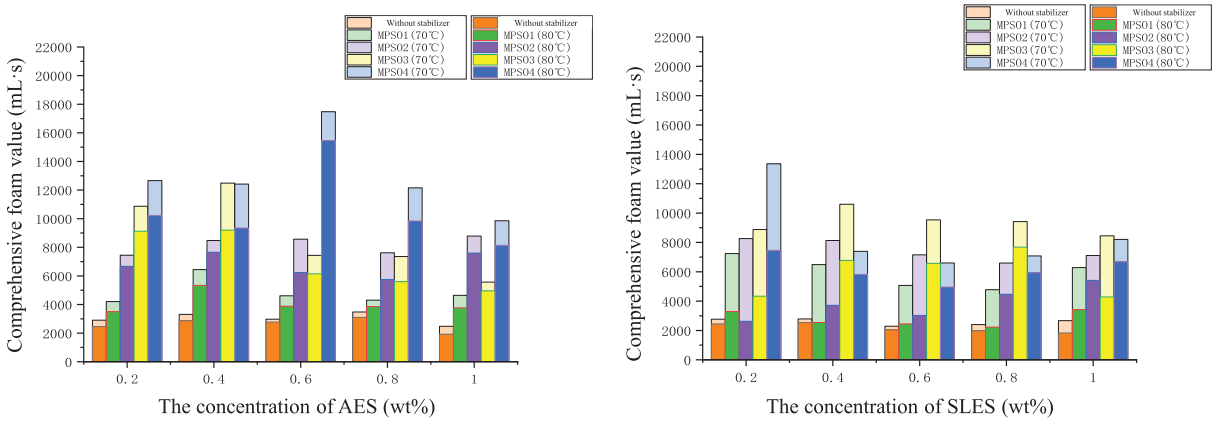

Figure 5: The comprehensive foam value of the anionic-nonionic surfactant foam system varies with the concentration of the surfactant and the type of microbial polysaccharide

Amphoteric surfactants carry both positive and negative charges, enabling them to interact synergistically with microbial polysaccharides without incompatibility issues due to electrostatic attraction [44]. We compounded lauryl betaine (LAB) and cocamidopropyl betaine (CAB) with microbial polysaccharides, and the results are shown in Fig. 6. The addition of microbial polysaccharides led to an improvement in foam stability, but the extent of improvement was significantly lower in the CAB system compared to the LAB system. The main reasons for this difference include: Firstly, LAB is an amphoteric surfactant with a molecular structure that includes a long alkyl chain and a betaine group. This structure allows LAB to form orderly arrangements at the gas-liquid interface rapidly, effectively reducing interfacial tension and promoting foam formation and stability. In contrast, cocamidopropyl betaine (CAB) molecules contain more amide groups, which make their molecular structure more complex and less likely to form orderly arrangements at the gas-liquid interface, leading to a poorer reduction in interfacial tension. Secondly, LAB has a higher HLB (Hydrophilic-Lipophilic Balance) value, enabling it to form tighter interactions with MPS04, thereby increasing the viscosity of the aqueous phase and the elasticity of the foam lamellae. This synergistic effect helps to form more stable foam lamellae, preventing the coalescence of droplets and thus enhancing foam stability. In comparison, the HLB value of cocamidopropyl betaine (CAPB) is lower, resulting in weaker interactions with MPS04, lower viscosity of the system, and less elastic foam lamellae, which lead to poorer foam stability. Additionally, the adsorption rate and adsorption amount of LAB at the gas-liquid interface are both higher, allowing it to quickly form a stable interfacial film and further enhance foam stability. Experimental results also demonstrate that the rheological properties of the system significantly improved when LAB was compounded with MPS04, as evidenced by increases in viscosity and elastic modulus. Conversely, the interfacial adsorption capacity of CAB is weaker, leading to poorer stability of the interfacial film and a shorter foam persistence time. Through optimization, the best system for microbial polysaccharides combined with amphoteric surfactants was determined to be: 0.4 wt% LAB + 0.08 wt% MPS04.

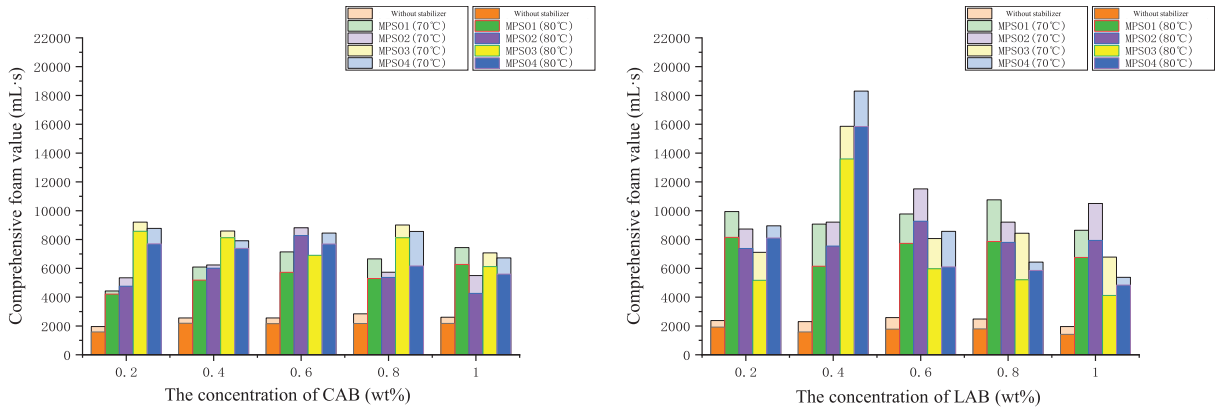

Figure 6: The comprehensive foam value of the amphoteric surfactant foam system varies with the concentration of the surfactant and the type of microbial polysaccharide

In summary, we have ultimately obtained three systems. The anionic surfactant foam system Formula (1): 0.6 wt% SDS + 0.08 wt% MPS04. The anionic-nonionic surfactant foam system Formula (2): 0.6 wt% AES + 0.08 wt% MPS04. The amphoteric surfactant foam system Formula (3): 0.4 wt% LAB + 0.08 wt% MPS04.

3.1.2 Optimized Salt Resistance

Foam fracturing fluids entering the reservoir will come into contact with formation water. High salinity formation water can affect the distribution of surfactants at the interface and the structure of microbial polysaccharides. Therefore, it is necessary to optimize the salt tolerance of the foam system to achieve the best high-temperature and high-salinity foam system.

To analyze the salt tolerance of the foam system selected in Section 3.1.1, a brine solution with a concentration of 250 g/L was prepared to simulate high-salinity formation water. The inorganic salt composition of the brine was as follows: Na_2SO_4 417, $NaHCO_3$ 756, NaCl 207,759, $CaCl_2$ 41,106, and $MgCl_2$ 3549 mg/L. When necessary, the brine was diluted to obtain salinities of 30, 60, and 90 g/L. As shown in Fig. 7, the stability of the foam system under different salinities was tested at 80°C using the same method. With the increase in salinity, the stability of foams from different systems generally decreased, primarily due to the curling of the MPS04 molecule in high-salinity environments, which weakens intermolecular interactions and reduces foam stability. Notably, the stability of the SDS foam system was most significantly affected by salinity, while that of the LAB foam system was the least affected, mainly due to the molecular structure of the foaming agents. The poor salt tolerance of SDS is primarily attributed to the strong interaction between its hydrophilic group (sulfate) and salt ions, which leads to salt precipitation at high salt concentrations. As the salt concentration increases, salt ions compete with the sulfate ions of SDS for water molecules, decreasing the solubility of SDS in water and thus affecting its surface activity. In contrast, AES, although also possessing a sulfate hydrophilic group, exhibits improved salt tolerance due to the presence of its polyoxyethylene ether segment, which enhances hydrophilicity. However, its salt tolerance is still inferior to that of LAB. LAB is an amphoteric surfactant, with both positively and negatively charged groups in its structure, allowing it to maintain good solubility and surface activity under different pH conditions. Additionally, the strong hydration effect in the betaine structure effectively reduces the impact of salt ions on its hydrophilic groups, enabling it to maintain high stability and surface activity even at high salt concentrations. Therefore, the LAB

foam system demonstrates the best salt tolerance. Taking all factors into consideration, the optimal foam system was determined to be 0.4 wt% LAB + 0.08 wt% MPS04.

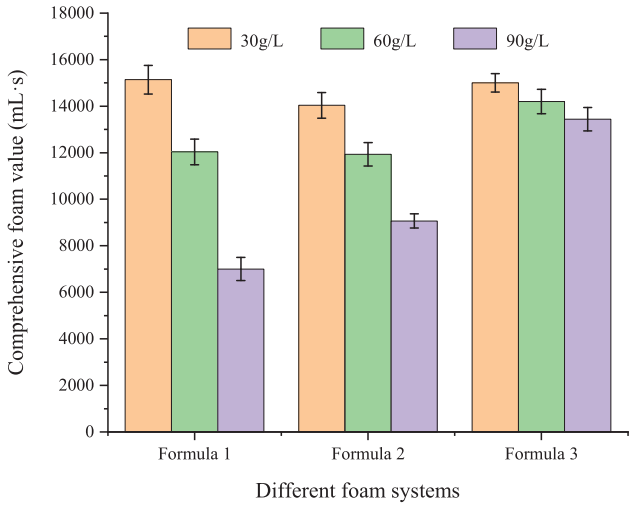

Figure 7: The comprehensive foam values of different foam systems vary with salinity

3.2 Performance Testing of Foam Fracturing Fluid

3.2.1 Static Proppant Suspension Test

The optimal system selected was tested for its proppant-carrying capacity. As shown in Fig. 8, in the absence of a foam stabilizer, the foam's proppant-carrying ability was very poor, and most of the proppant settled to the bottom of the foam within 30 min.

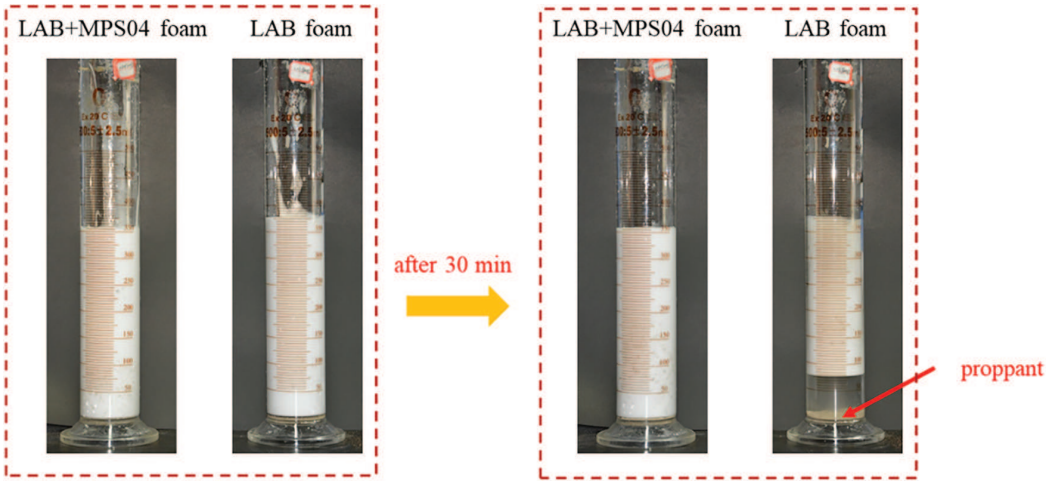

Figure 8: Settlement of proppant within foam fracturing fluid

To further analyze the static proppant suspension performance of the foam system, we statistically evaluated the changes in liquid separation volume and proppant settlement volume over time, as shown in Fig. 9. In Fig. 9A, it can be observed that in the absence of the MPS04 foam stabilizer, the foam generated

solely by LAB has a liquid separation half-life of approximately 5 min, with an initial foam height of 347 mL. However, in the foam system with the addition of the stabilizer, only 4 mL of liquid separation occurred by the end of the experiment, which represents just 4% of the 100 mL base fluid volume. Such performance is particularly noteworthy at a high salinity of 90 g/L. Additionally, as illustrated in Fig. 9B, at a high salinity of 90 g/L, the pure LAB foam ruptures rapidly, resulting in very poor proppant suspension. The proppant settlement rate reaches 84% within 15 min and exceeds 90% after 30 min. The proppant settlement trend is almost consistent with the liquid separation trend of the foam. When the MPS04 foam stabilizer is added, the proppant settlement rate significantly decreases, with only 18% settlement occurring even at 60 min, fully meeting the requirements for proppant-carrying capacity in fracturing operations.

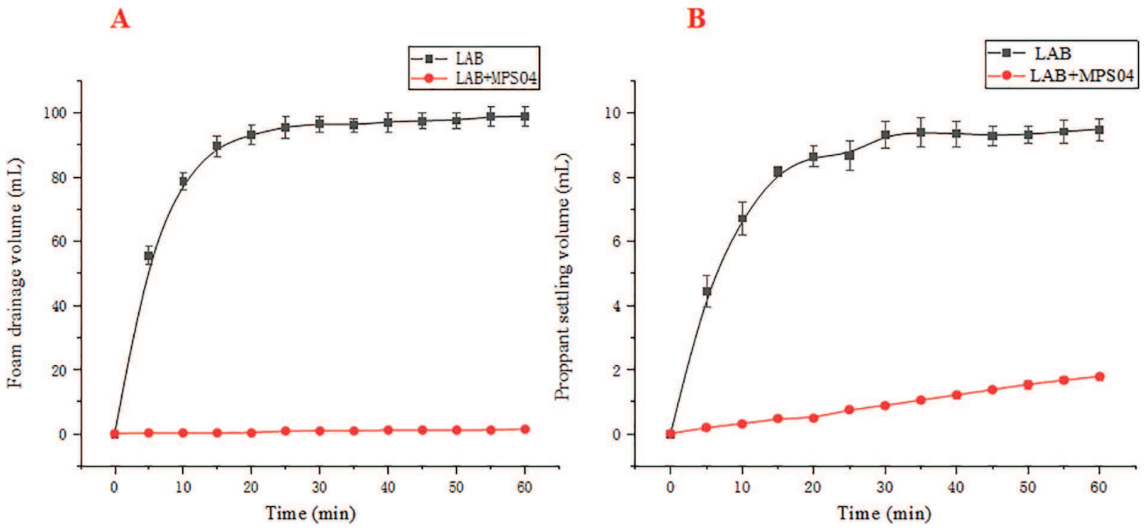

Figure 9: Changes in foam drainage and proppant settlement over time. (A: Foam drainage; B: Proppant settlement)

3.2.2 Dynamic Proppant Carrying Capacity Test

The Fig. 10 illustrates the distribution of proppant in a flat plate during the injection process. From Fig. 10, it can be observed that in the LAB foam, the proppant concentration is higher at the front end, while it significantly decreases in the latter half, indicating severe foam drainage and poor dynamic proppant-carrying capacity. In contrast, the LAB+MPS04 foam shows a uniform distribution of proppant throughout the flat plate, and the foam remains stable throughout the injection process with no significant foam drainage. This suggests that the addition of the MPS04 foam stabilizer improves the proppant-carrying capacity of the foam, allowing proppant to be transported deeper into the fractures, thereby enhancing the fracture conductivity and improving the overall fracturing efficiency [45].

3.2.3 Core Damage Test

Table 2 presents the damage results of the fracturing fluids. The permeability damage rate ηd of the conventional guar gum fracturing fluid is approximately 33.56%, while the damage rate of the LAB+MPS04 foamed fracturing fluid on the core is 19.43%. The insoluble residues from the guar gum fracturing fluid block the pore throats of the formation, whereas the microbial polysaccharide foam, due to its extremely low usage, causes significantly less damage to the reservoir.

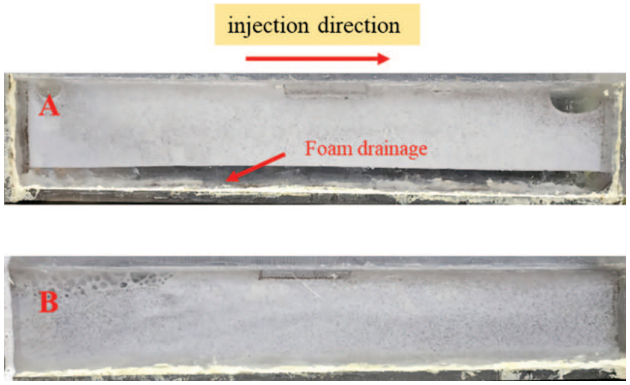

Figure 10: Sand-carrying performance during the foam injection process. (A: LAB foam, B: LAB+MPS04 foam)

Table 2: The damage of fracturing fluids on core permeability

Fracturing fluid types	Permeability mD		Core damage rate %
	K_1	K_2	
LAB+MPS04	10.86	8.75	19.43
guar gum fracturing fluid	23.27	15.46	33.56

3.3 Study on Foam Stabilization Mechanism

3.3.1 Foam Coarsening

The foam was placed on a microscope slide, and its size and quantity were observed under a microscope from the time of preparation until 1 h had elapsed (at a magnification of 100 times), as shown in Fig. 11.

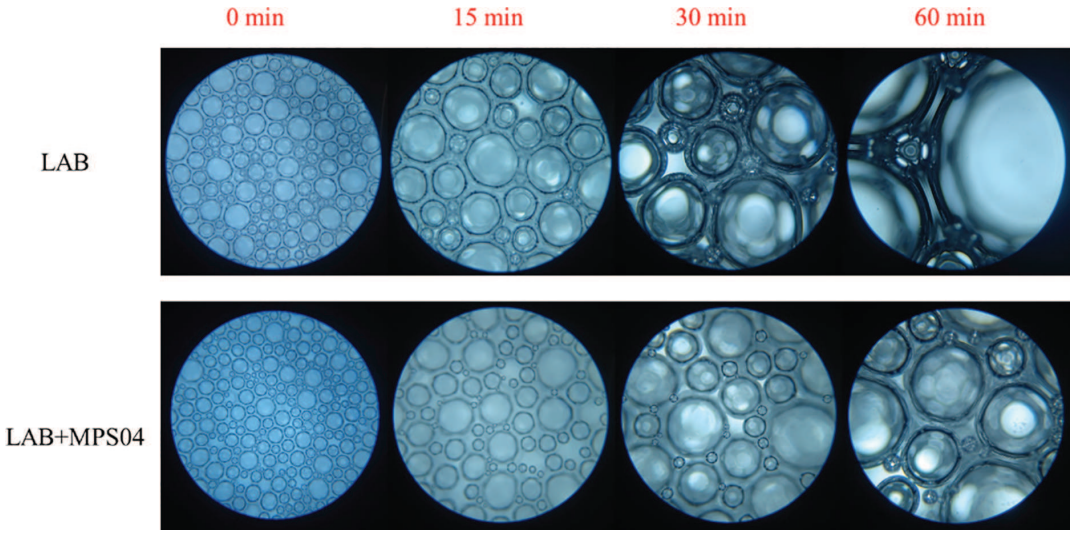

Figure 11: The variation in foam quantity and bubble size over time

At the beginning, the volume and density of the foam generated by LAB alone and that generated by LAB+MPS04 showed little difference, indicating that the addition of the foam stabilizer had no significant effect on foam size. By 15 min, a noticeable difference in foam radius between the single and composite

systems began to emerge. The radius of the foam in the single system was larger, and the number of foam bubbles within the field of view was fewer, with a significant change in foam volume compared to the initial state. In contrast, the foam diameter in the composite system was smaller, and the foam remained relatively dense, although many larger diameter bubbles began to appear. Most of the bubbles were still small, and the volume change was less pronounced compared to the initial state, indicating better stability of the LAB foam. At 30 and 60 min, the difference in foam diameter between the two systems became even more evident. To further analyze the foam-stabilizing effect of MPS04, the average diameter of the foam bubbles in each microscopic image was calculated using the ImageJ image processing tool. The statistical results are presented in Fig. 12.

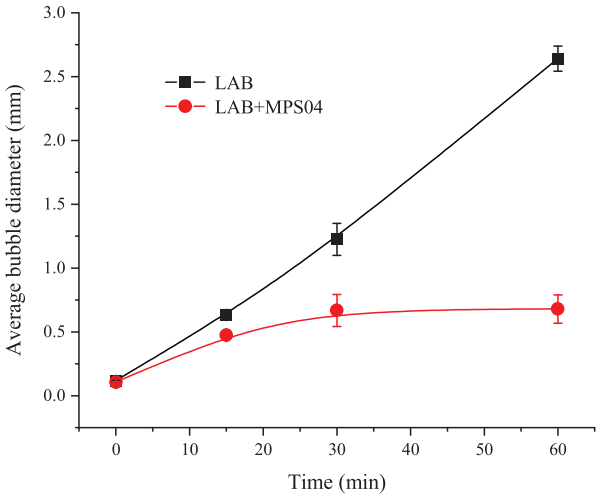

Figure 12: The variation in average foam diameter over time

As shown in the Fig. 12, the radius of the SDS foam changes over time with a slope that is nearly linear, whereas the foam radius in the system with the MPS04 foam stabilizer exhibits a more gradual slope, indicating a significant improvement in foam stability. We hypothesize that this phenomenon is due to the formation of a network structure by the MPS04 molecules within the liquid film. The presence of this network structure significantly increases the viscosity of the liquid film, thereby slowing down the drainage and coarsening of the foam, which enhances foam stability. To verify the formation of the network structure, we conducted scanning electron microscopy (SEM) analysis of the liquid film structure, as shown in Fig. 13. The SEM images reveal that complex network structures are indeed formed by MPS04 within the liquid film, confirming the accuracy of our hypothesis.

3.3.2 Foam Viscoelasticity

As shown in Fig. 14, the foam viscoelasticity is tested by measuring the frequency dependence of the storage modulus (G′) and loss modulus (G″). In the case of foam containing only LAB, the storage modulus is greater than the loss modulus at low frequencies, indicating that the foam is predominantly elastic. However, as the frequency increases, the loss modulus exceeds the storage modulus, suggesting that the foam becomes more viscous. After adding MPS04, the elastic properties of the foam are significantly enhanced, and the storage modulus remains higher even at higher frequencies, indicating a more pronounced elastic nature. Comparing the results before and after the addition of MPS04, it is evident that the storage modulus of the foam increases significantly upon the addition of MPS04, suggesting that the primary effect of MPS04 is

on the storage modulus of the system. The reason for this is the strong electrostatic interaction between MPS04 and LAB, which causes a significant portion of MPS04 to adsorb onto the liquid film surface. This results in the foam being enveloped by MPS04, and the formation of a network structure by MPS04 in the solution significantly increases the viscoelasticity of the solution. Therefore, when MPS04 is present at the interface, it also forms a network structure, thereby reinforcing the viscoelasticity of the foam. By comparing Fig. 14a and b, it is clear that the storage modulus of the foam system increases with the addition of MPS04. The storage modulus characterizes the ability of the interfacial film to resist deformation; a higher storage modulus indicates a stronger resistance to external disturbances and is beneficial for enhancing foam stability [40,46]. Additionally, the increase in the storage modulus after adding MPS04 enhances the foam's resistance to external disturbances, reduces the settling of proppant within the foam, and improves the foam's ability to carry proppant. This verifies the reason for the enhanced sand-carrying capacity of the foam.

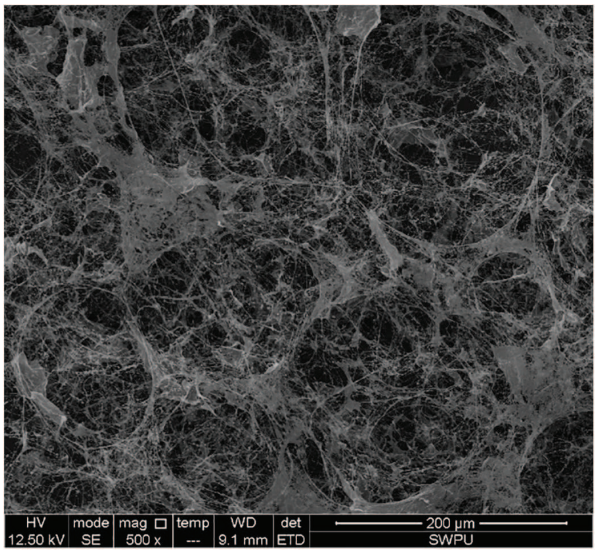

Figure 13: The microstructure of the foam

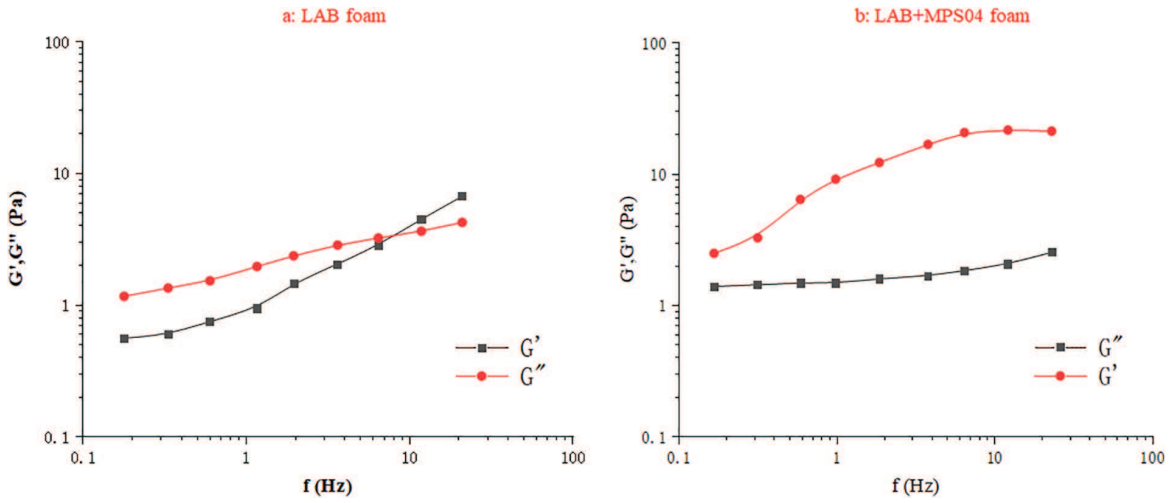

Figure 14: The variation of foam modulus with scanning frequency (a: LAB form, b: LAB+MPS04 form)

4 Conclusion

(1) Based on the Waring-blender method, with the comprehensive foam performance as the evaluation criterion, the optimal combinations of different types of surfactants and microbial polysaccharides were selected under high-temperature conditions. The results indicate that the optimal formulation for the anionic surfactant foam system is 0.6 wt% SDS + 0.08 wt% MPS04; for the anionic-nonionic surfactant foam system, it is 0.6 wt% AES + 0.08 wt% MPS04; and for the zwitterionic surfactant foam system, it is 0.4 wt% LAB + 0.08 wt% MPS04.

(2) To further optimize the salt-tolerant foaming fracturing fluid system, the foam system was further optimized under high salinity conditions. The results show that at a salinity of 90 g/L, the 0.4 wt% LAB + 0.08 wt% MPS04 system exhibits the best comprehensive foam performance. The salt tolerance of the foam systems is in the order: SDS < AES < LAB, which is mainly attributed to the structural differences of the surfactant molecules. Salt ions compete with the sulfonate groups of SDS for water molecules, reducing the solubility of SDS in water and thus affecting its surface activity. In contrast, although AES also has sulfonate hydrophilic groups, the presence of polyoxyethylene ether segments increases its hydrophilicity, thereby enhancing its salt tolerance. LAB, a zwitterionic surfactant, possesses both positively and negatively charged groups in its structure, allowing it to maintain good solubility and surface activity under different pH conditions. Additionally, the strong hydration effect in the betaine structure effectively reduces the impact of salt ions on its hydrophilic groups, ensuring high stability and surface activity even at high salt concentrations.

(3) After adding MPS04, the foam stability of the fracturing fluid was significantly enhanced, and the sand-carrying capacity of the foam was markedly improved. At 60 min, the proppant settling volume was only 18%. Dynamic sand-carrying tests also indicated that the LAB + MPS04 foam maintained a uniform distribution of proppant on the flat plate during injection and remained stable throughout the process. This allows the foam to carry proppant deeper into the fractures, thereby improving the fracturing efficiency. Simultaneously, this foam system exhibits lower formation damage compared to conventional guar gum foam fracturing fluids, making it highly suitable for productivity enhancement in unconventional reservoirs.

(4) The addition of MPS04 results in the formation of a complex network structure within the liquid film, which effectively inhibits foam coarsening and enhances foam stability. Additionally, this network structure strengthens the foam lamellae, improving the viscoelasticity of the foam. Consequently, it ensures the excellent sand-carrying performance of the foam.

In conclusion, this study innovatively developed a microbial polysaccharide and surfactant blended foam fracturing fluid system, investigating its foam stabilization mechanism and key performance characteristics. The system exhibits significant foam stability, excellent sand-carrying capacity, and low core damage, especially performing well under high temperature and high salinity conditions. Microbial polysaccharides enhance the viscoelasticity of the foam liquid films, significantly improving foam stability. Additionally, the network structure formed by the foam stabilizer in the liquid film effectively suppresses foam coarsening, enhancing both foam stability and sand-carrying capacity. Although the blended system demonstrates good performance in laboratory experiments, its thermal stability under extreme conditions still requires further optimization. Field conditions are complex, and the fracturing fluid system may face contamination from oil phases, CO_2, SO_2, and other substances in the reservoir. Future research should focus on improving the system's adaptability under field conditions and exploring its application potential in more complex reservoir environments. Furthermore, microbial polysaccharides are high molecular weight materials, and their degradation in reservoir environments will also be an important issue for future studies.

Acknowledgement: Thanks to China National Petroleum Corporation for supporting this work.

Funding Statement: This study was supported by the Key Technology Research on Increasing Recovery Rate in Tight Sandstone Gas Reservoirs, a Major Scientific and Technological Special Project of China National Petroleum Corporation (Project No. 2023ZZ25).

Author Contributions: The authors confirm contribution to the paper as follows: study conception and design: Zhiqiang Jiang, Zili Li; data collection: Bin Liang, Miao He; analysis and interpretation of results: Weishou Hu, Jun Tang; draft manuscript preparation: Chao Song, Nanxin Zheng. All authors reviewed the results and approved the final version of the manuscript.

Availability of Data and Materials: The data that support the findings of this study are available from the corresponding author upon reasonable request.

Ethics Approval: Not applicable.

Conflicts of Interest: The authors declare no conflicts of interest to report regarding the present study.

References

1. Newell R, Raimi D, Villanueva S. Global energy outlook 2020: energy transition or energy addition. Resour Future. 2020;7:132–9. doi:10.24112/jaes.070010.
2. Kober T, Schiffer HW, Densing M, Panos E. Global energy perspectives to 2060-WEC's world energy scenarios 2019. Energy Strategy Rev. 2020;31:100523. doi:10.1016/j.esr.2020.100523.
3. Karimidastenaei Z, Avellán T, Sadegh M. Unconventional water resources: global opportunities and challenges. Sci Total Environ. 2022;827(3):154429. doi:10.1016/j.scitotenv.2022.154429.
4. Mansi AE, El-Marsafy SM, Elhenawy Y. Assessing the potential and limitations of membrane-based technologies for the treatment of oilfield produced water. Alex Eng J. 2023;68(33):787–815. doi:10.1016/j.aej.2022.12.013.
5. Muther T, Qureshi HA, Syed FI, Aziz H, Siyal A, Kalantari D, et al. Unconventional hydrocarbon resources: geological statistics, petrophysical characterization, and field development strategies. J Pet Explor Prod Te. 2022;12(6):1463–88. doi:10.1007/s13202-021-01404-x.
6. Li Y, Xu Y. Recent advances in tight oil reservoir development: integrated technology of horizontal drilling and hydraulic fracturing. Adv Resour Res. 2024;4(3):300–17. doi:10.1021/es405118y.
7. Jew AD, Druhan JL, Ihme M, Anthony R, Iienia B, John K, et al. Chemical and reactive transport processes associated with hydraulic fracturing of unconventional oil/gas shales. Chem Rev. 2022;122(9):9198–263. doi:10.1021/acs.chemrev.1c00504.
8. Lin W. A review on shale reservoirs as an unconventional play—the history, technology revolution, importance to oil and gas industry, and the development future. Acta Geologica Sinica-Eng Ed. 2016;90(5):1887–902. doi:10.1111/1755-6724.12823.
9. Vengosh A, Jackson RB, Warner N, Darrah T, Kondash A. A critical review of the risks to water resources from unconventional shale gas development and hydraulic fracturing in the United States. Environ Sci Technol. 2014;48(15):8334–48. doi:10.1021/es405118y.
10. Davoodi S, Al-Shargabi M, Wood DA. Geothermal energy recovery from abandoned petroleum wells: a review of the challenges and opportunities. Sustian Energy Techn. 2024;68:103870. doi:10.1016/j.seta.2024.103870.
11. Detournay E. Slickwater hydraulic fracturing of shales. J Fluid Mech. 2020;886:514–50. doi:10.1017/jfm.2019.1023.
12. Srinivas B, Sreekanth T. Eco-friendly guar gum composites as solid-state electrolytes. Mater Chem Phys. 2024;320(21):129453. doi:10.1016/j.matchemphys.2024.129453.
13. Barati R, Liang JT. A review of fracturing fluid systems used for hydraulic fracturing of oil and gas wells. J Appl Polym Sci. 2014;131(16):327. doi:10.1002/app.40735.

14. Davoodi S, Al-Shargabi M, Wood DA, Rukavishnikov V. A comprehensive review of beneficial applications of viscoelastic surfactants in wellbore hydraulic fracturing fluids. Fuel. 2023;338:127228. doi:10.1016/j.fuel.2022.127228.
15. Meshram PD, Shingade S, Madankar CS. Comparative study of saponin for surfactant properties and potential application in personal care products. Mater Today: Proc. 2021;45(3):5010–3. doi:10.1016/j.matpr.2021.01.448.
16. Ratzer AF. History and development of foam as a fire extinguishing medium. Ind Eng Chem Res. 1956;48(11):2013–6. doi:10.1021/ie50563a030.
17. Suparanon T, Phetwarotai W. Fire-extinguishing characteristicsand flame retardant mechanism of polylactide foams: influence of tricresyl phosphate combined with natural flame retardant. Int J Biol Macromol. 2020;158:1090–101. doi:10.1016/j.ijbiomac.2020.04.131.
18. Micheau C, Schneider A, Girard L. Evaluation of ion separation coefficients by foam flotation using a carboxylate surfactant. Colloid Surf A. 2015;470:52–9. doi:10.1016/j.colsurfa.2015.01.049.
19. Blauer RE, Mitchell BJ, Kohlhaas CA. Determination of laminar, turbulent, and transitional foam flow losses in pipes. In: SPE Western Regional Meeting; 1974 Apr 4–5; San Francisco, CA, USA. p. SPE-4885. doi:10.2118/4885-MS.
20. Blauer RE, Kohlhaas CA. Formation fracturing with foam. In: SPE Western Regional Meeting; 1974 Apr 4–5; San Francisco, CA, USA. p. SPE-5003 doi:10.2118/5003-MS.
21. Faroughi SA, Pruvot AJCJ, McAndrew J. The rheological behavior of energized fluids and foams with application to hydraulic fracturing. J Petrol Sci Eng. 2018;163(6):243–63. doi:10.1016/j.petrol.2017.12.051.
22. Sun Q, Li Z, Wang J, Li S, Li B, Jiang L, et al. Aqueous foam stabilized by partially hydrophobic nanoparticles in the presence of surfactant. Colloid Surface A. 2015;471:54–64. doi:10.1016/j.colsurfa.2015.02.007.
23. AlYousef ZA, Almobarky MA, Schechter DS. The effect of nanoparticle aggregation on surfactant foam stability. J Colloid Interf Sci. 2018;511(5):365–73. doi:10.1016/j.jcis.2017.09.051.
24. Rafati R, Haddad AS, Hamidi H. Experimental study on stability and rheological properties of aqueous foam in the presence of reservoir natural solid particles. Colloid Surface A. 2016;509:19–31. doi:10.1016/j.colsurfa.2016.08.087.
25. Wang J, Chen Y, Wang S, Liu H, Zhao F. Investigations on the influencing mechanisms of SiO_2 nanoparticles on foam stability. Energy Fuels. 2021;35(24):20016–25. doi:10.1021/acs.energyfuels.1c02975.
26. Ab Rasid SA, Mahmood SM, Kechut NI, Akbari S. A review on parameters affecting nanoparticles stabilized foam performance based on recent analyses. J Petrol Sci Eng. 2022;208(2):109475. doi:10.1016/j.petrol.2021.109475.
27. Emrani AS, Nasr-El-Din HA. An experimental study of nanoparticle-polymer-stabilized CO_2 foam. Colloids Surfaces A. 2017;524:17–27. doi:10.1016/j.colsurfa.2017.04.023.
28. Pal NA, Kumar N, Yaseri A, Ali M, Ojha K. Nanoparticles stabilized foam fluid for hydraulic fracturing application of unconventional gas reservoirs: a review of the properties, progress and future prospects. Petroleum Res. 2024;26(8):5335. doi:10.1016/j.ptlrs.2024.08.004.
29. Pandey S, Kannaujiya VK. Bacterial extracellular biopolymers: eco-diversification, biosynthesis, technological development and commercial applications. Int J Biol Macromol. 2024;279:135261. doi:10.1016/j.ijbiomac.2024.135261.
30. Nambiar K, Saravana Kumari K, Devaraj D, Sevanan M. Development of biopolymers from microbes and their environmental applications. Phys Sci Rev. 2024;9(4):1903–29. doi:10.1515/psr-2022-0219.
31. Bilal M, Iqbal HMN. Biologically active macromolecules: extraction strategies, therapeutic potential and biomedical perspective. Int J Biol Macromol. 2020;151(4):1–18. doi:10.1016/j.ijbiomac.2020.02.037.
32. Jindal N, Khattar JS. Microbial polysaccharides in food industry. J Biotechnol. 2016;231:38. doi:10.1016/j.jbiotec.2016.05.151.
33. Kang W, Yan L, Ding F, Xu Z. Effect of polysaccharide polymers on the surface and foam properties of aqueous film-forming foam. Colloid Interfac Sci. 2021;45:100540. doi:10.1016/j.colcom.2021.100540.
34. Pu W, Wei P, Sun L, Jin F, Wang S. Experimental investigation of viscoelastic polymers for stabilizing foam. J Ind Eng Chem. 2017;47(1):360–7. doi:10.1016/j.jiec.2016.12.006.

35. Verma A, Chauhan G, Ojha K. Characterization of α-olefin sulfonate foam in presence of cosurfactants: stability, foamability and drainage kinetic study. J Mol Liq. 2018;264(2):458–69. doi:10.1016/j.molliq.2018.05.061.
36. Tiong ACY, Tan IS, Foo HCY. A mechanistic study of surfactants, particles, and polymers on Foam stabilization. IOP Conf Ser Mater Sci Eng. 2019;495(1):012058.
37. Xu L, Xu G, Yu L, Gong H, Dong M, Li Y. The displacement efficiency and rheology of welan gum for enhanced heavy oil recovery. Polym Advan Technol. 2014;25(10):1122–9. doi:10.1088/1757-899X/495/1/012058.
38. Moscovici M. Present and future medical applications of microbial exopolysaccharides. Front Microbiol. 2015;6(189):1012. doi:10.3389/fmicb.2015.01012.
39. Khormali A, Petrakov D, Farmanzade A. Prediction and inhibition of inorganic salt formation under static and dynamic conditions—effect of pressure, temperature, and mixing ratio. Int J Technol. 2016;6(6):943–51. doi:10.14716/ijtech.v7i6.2871.
40. Niu Q, Dong Z, Lv Q, Zhang F, Shen H, Yang Z, et al. Role of interfacial and bulk properties of long-chain viscoelastic surfactant in stabilization mechanism of CO_2 foam for CCUS. J CO_2 Util. 2022;66:102297.
41. Kang W, He Y, Li Z, Yang H, Ye Z, Li W, et al. Stability mechanisms of viscoelastic zwitterionic-anionic surfactants enhanced foam system for low-permeability reservoirs. J Mol Liq. 2023;369:120883. doi:10.1016/j.molliq.2022.120883.
42. Pang Z, Wu Y, Zhao M. Novel evaluation method of foam agents for thermal recovery in heavy oil reservoirs. Energy Fuels. 2016;30(4):2948–57. doi:10.1021/acs.energyfuels.6b00455.
43. Kalam S, Afagwu C, Al Jaberi J, Osama S, Tariq M, Muhammad Z. A review on non-aqueous fracturing techniques in unconventional reservoirs. J Nat Gas Sci Eng. 2021;95:104223. doi:10.1016/j.jngse.2021.104223.
44. Verma C, Goni LKMO, Yaagoob IY, Vashisht H, Mazumder M, Alfantazi A. Polymeric surfactants as ideal substitutes for sustainable corrosion protection: a perspective on colloidal and interface properties. Adv Colloid Interfac. 2023;318:102966. doi:10.1016/j.cis.2023.102966.
45. Schechter D. Investigating the effect of improved fracture conductivity on production performance of hydraulically fractured wells: field-case studies and numerical simulations. J Can Petrol Technol. 2015;54(6):442–9. doi:10.2118/169866-PA.
46. Moradpour N, Yang J, Tsai PA. Liquid foam: fundamentals, rheology, and applications of foam displacement in porous structures. Curr Opin Colloid In. 2024;74:101845. doi:10.1016/j.cocis.2024.101845.